INVESTIGATION OF PLANE ELASTIC–PLASTIC PROBLEMS BY THE HOLOGRAPHIC INTERFEROMETRY METHODS

S. I. Gerasimov and V. A. Zhilkin

UDC 620.171.5

When solving elastic–plastic problems, the idealization taken for the properties of the deformable medium and especially the boundary conditions frequently do not permit reliable consideration of the results obtained according to the theoretical solutions of the mechanics of plastic body molding (if they exist) corresponding to a real process.

In this connection an important role belongs to experimental investigations during whose execution full-scale boundary conditions are successfully realized and information is obtained about the displacement fields of the surface sections being studied on real articles. Among such methods, in particular, is the method of holographic interferometry (HIM) which is successfully used at this time to solve nondestructive control problems, elasticity theory, vibration theory problems, and certain plasticity theory problems [1-7].

Known HIM applications are described in this paper for the solution of elastic–plastic beam and plate deformation problems and certain new results are presented that illustrate the possibilities of this optical method and those difficulties which may be encountered by the experimenter when obtaining quantitative information about the article deformation process. We shall everywhere henceforth use the standard notation in elasticity theory for the projections U, V, and W of the displacement vector Δr on the Cartesian x, y, z coordinate axes, respectively. The z axis agrees in direction with the external normal to the article surface.

1. HOLOGRAPHIC INTERFEROMETRY METHODS IN EXPERIMENTAL MECHANICS

The displacement W of diffuse surface points of articles is successfully determined qualitatively easily and with high accuracy by the holographic interferometry method (HIM). In classical hologram recording schemes the recording medium and the object of investigation are separated from each other by a considerable distance in space, which specifies the need to apply specialized vibrations-insulating test-stands (of the type of SIN, UIG, VIS, etc.) in connection with the high sensitivity of the method to the mutual displacement, and it imposes rigid requirements on the level of article displacement as an absolutely solid body, which are "noisy" in this case, making difficult the analysis of the deformed state of the body surface section being studied. In its turn this does not permit the utilization of standard equipment to load the articles and obliges the experimenters to fabricate special loading adapters or to investigate just those problems in which the displacements of the body being tested as a rigid whole are known not to be large.

Consequently, the majority of the first researches is devoted to a study of the strain state of flexible cantilever beams and plates with a rigidly clamped contour [8-13] or plane short specimens subjected to tension for which a zone of zero displacements [14, 15] is assumed near the specimen surface section being studied by different technical methods. A qualitative analysis of the interference patterns was performed in the majority of the listed papers and just the function W(x, y) was determined experimentally. Papers [8, 9] in which quantitative results on determining the residual stresses in ground and riveted layers of a beam from the alloy ÉI 617, obtained as a result of numerical processing of experimental information during which the third derivative of the function W(x, y) should be evaluated, come out of this series.

The first attempt to determine all three projections of the displacement vector Δr on the coordinate axes from information obtained by using HIM was made by the authors of [16],

Novosibirsk. Translated from Zhurnal Prikladnoi Mekhaniki i Tekhnicheskoi Fiziki, No. 2, pp. 107-115, March-April, 1988. Original article submitted November 4, 1986.

 0021-8944/88/2902-0260$12.50

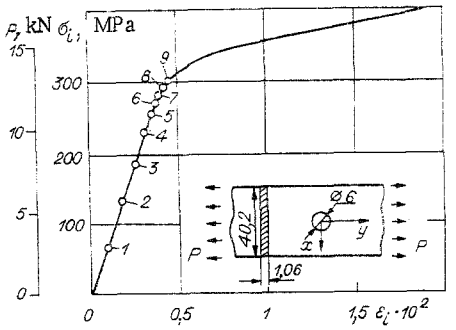

Fig. 1

who assumed that the displacement fields U(x, y), V(x, y), W(x, y) could be determined separately by experimental means by an appropriate selection of the hologram recording directions.

It is known at this time that this problem cannot be solved by using holographic interferometry. The HIM permits information to be obtained about the level lines of just the function W(x, y) while the isophasal surfaces (or interference fringe patterns) in the remaining cases are determined by a combination of two or three projections of the displacement vector $\Delta \mathbf{r}$.

In the general case the resolving equation of the holographic interferometry method has the form [5]

$$\Delta \mathbf{r} \cdot (\boldsymbol{\rho}_o - \boldsymbol{\rho}_e) = N\lambda, \tag{1.1}$$

where $\Delta \mathbf{r} = U\mathbf{i} + V\mathbf{j} + W\mathbf{k}$; $\boldsymbol{\rho}_o$, $\boldsymbol{\rho}_e$ are unit vectors of the observation and exposure directions of points of the object, $\boldsymbol{\rho}_o = \mathbf{i}\cos\alpha_o + \mathbf{j}\cos\beta_o + \mathbf{k}\cos\gamma_o$, $\boldsymbol{\rho}_e = \mathbf{i}\cos\alpha_e + \mathbf{j}\cos\beta_e + \mathbf{k}\cos\gamma_e$; α_m, β_m, γ_m ($m = o, e$) are angles between the unit vector of the direction o or e and the x, y, z coordinate axes, respectively, N is the order of the interference fringes, and λ is the radiation wavelength of the light source being used.

It follows from (1.1) that only in the case of symmetry of the exposure and observation directions beyond the point of the object relative to the normal to the specimen surface will the order of the interference fringes (isophasal lines) became proportional to the displacement function

$$W = N\lambda/2\cos\gamma, \tag{1.2}$$

while in the remaining cases (1.1) will contain two or three projections of the desired displacement vector for whose determination two or three equations of the type (1.1) must be solved jointly.

The quantity of publications on theme under discussion did not increase substantially in the 80's, the class of solvable problems was not expanded but the accent in the majority of papers was on the development of recipes and methods to obtain quantitative information about the processes being investigated [17-20].

The reasons delaying wider insertion of the HIM into experimental mechanics in its classical version with the recording medium and the object under investigation separated in space are:

the impossibility of utilizing standard test equipment because of unallowably high displacements of the object being studied as a rigid whole relative to the recording medium in the time interval between two exposures of the photographic material. The vibrations of the standard test equipment do not permit realization of a high-quality hologram recording;

the low accuracy of determining the functions U(x, y), V(x, y) from a system of the type (1.1) from the data of decoding just one interferogram because of its small aperture angle or several interferograms because of difficulties in numbering the interference fringes.

Free of the listed disadvantages are the holographic interferometers applied [21, 22] in which in order to reduce the demands on insulating the vibrations of the experimental set-up elements and to raise the accuracy of determining the strains the photorecording medium is

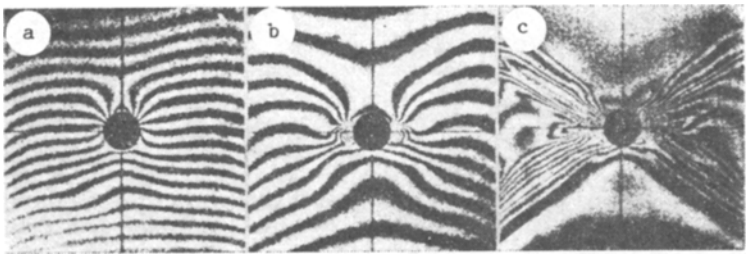

Fig. 2

fastened to the surface of the article being studied [23] and the holographic interferograms are recorded in opposite beams [24].

2. APPLIED INTERFEROMETERS

When studying the strain state of massive articles the recording medium on their surface can be fastened mechanically or by magnetic springs [23, 25] or by using an optically transparent, nonpiezosensitive rubberlike medium with a small shear stiffness [22]. We use only the last of the methods listed in studying thin-walled structures. In this case the resolving equation of HIM has the form $U\cos\alpha_k + V\cos\beta_k + W(n + \sqrt{n^2 - \sin^2\gamma_k}) = N\lambda$, upon exposure of the object to a plane coherent wave normally incident on the photographic plate, where n is the index of refraction of the intermediate transparent medium, and k is a subscript characterizing the different directions of observation.

If the interference patterns are recorded from four pairwise symmetrical directions relative to the z axis (k = 1, 2, 3, 4) that lie in two mutually perpendicular planes x0z and y0z, then the projections U, V, and W of the displacement vector Δr of points of the article surface can be found from the formulas:

The directions of observation 1 and 2 lie in the y0z plane

$$V = \lambda(N_1 - N_2)/2\cos\beta_{1,2}; \tag{2.1}$$

$$W = \lambda(N_1 + N_2)/(n + \sqrt{n^2 - \sin^2\gamma_{1,2}}); \tag{2.2}$$

The directions of observation 3 and 4 lie in the x0z plane

$$U = \lambda(N_3 - N_4)/2\cos\alpha_{3,4}; \tag{2.3}$$

$$W = \lambda(N_3 + N_4)/(n + \sqrt{n^2 - \sin^2\gamma_{3,4}}). \tag{2.4}$$

Determination of the projection W from the depencences (2.2) and (2.4) requires knowledge of the absolute refractive index n which complicates somewhat the decoding process as compared with the utilization of relationship (1.2). Consequently, the applied interferometers are used mainly to determine the planar displacements U(x, y) and V(x, y).

The interferomogram is the transducer of the mechanical quantities (displacement) into an optical signal in the HIM. The range of strains measurable by using such a transducer

$$D = (\min\psi_i \ldots \max\psi_i)/S \tag{2.5}$$

is inversely proportional to its sensitivity

$$S_U = \cos\alpha_{3,4}/\lambda,\ S_V = \cos\beta_{1,2}/\lambda, \tag{2.6}$$

where max ψ_i, min ψ_i are the maximal and minimal interference pattern frequencies determined by the averaging level of the strains on the basis of the interference fringes and the technical characteristics of the equipment being used (most often min ψ_i = 0.05 lines/mm and max ψ_i = 1 line/mm). The numerator in (2.5) is independent of the optical method being used.

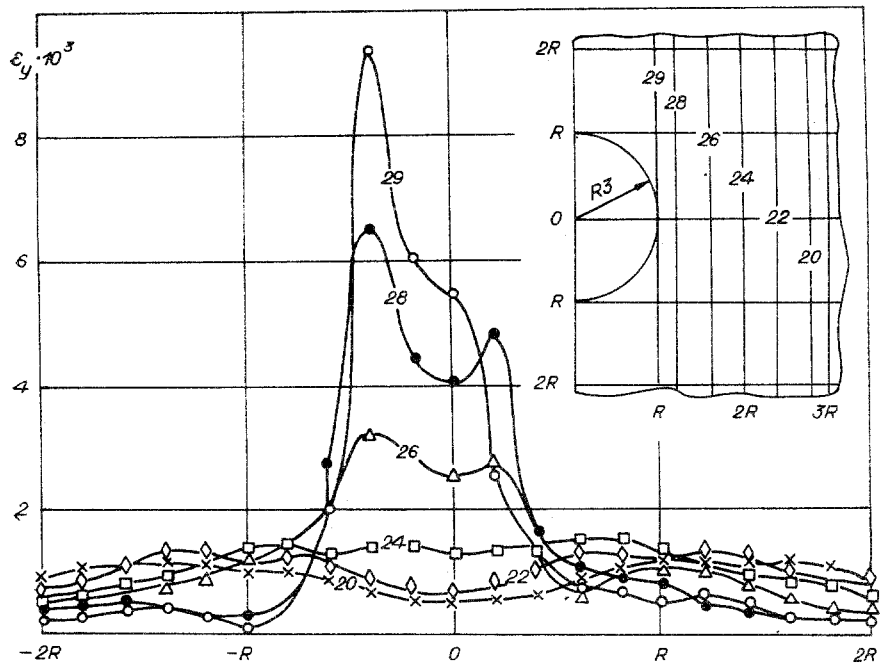

Fig. 3

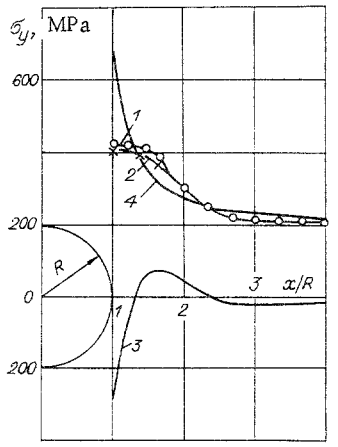

Fig. 4

Taking into account the fact that $\lambda = 0.6328$ for the most extensively utilized He–Ne laser, the dependence of the range of strains measurable by HIM on the transducer sensitivity is written in the form

$$D = (3—63)\cdot 10^{-5}/\cos\alpha. \qquad (2.7)$$

Under real conditions the angle α cannot equal zero (in this case the direction of observation is oriented along the photographic plate surface) and should not equal 90° because then the interferometer sensitivity to the projection of the displacement vector lying in the tangent plane is zero. For α close to 90° the sensitivity of the interferometer to the displacement U (see (2.6)) can be ten times less than the sensitivity to the displacement W (here $\alpha = 90° - \gamma$ is taken): $S_W/S_U = (n + \sqrt{n^2 - \sin^2\gamma})/\sin\gamma$. Thus, $S_W/S_U \approx 17$ for $n = 1.5$ and $\gamma = 10°$.

Consequently, α is ordinarily chosen within the limits 30-60°. For $\alpha = 60°$ ($S_U = 790$ lines/mm), $D = 6\cdot 10^{-5}$-$2\cdot 10^{-3}$, i.e., by using such a transducer only elastic problems of the mechanics of a deformable medium can be investigated or it can be used when studying plastic deformation processes of the article material in combination with other optical methods possessing a lower sensitivity. Application of HIM as an independent device specifies the necessity to use step-by-step methods of both specimen loading and interference pattern

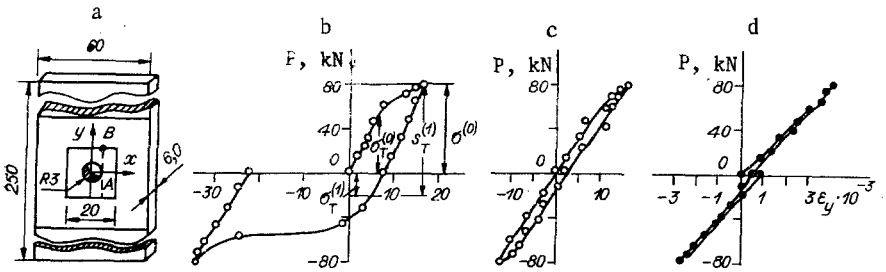

Fig. 5

inscription. For instance, if it is required to study the strain state of a strip fabricated from the naterial D16P and tested for central tension, then it is required to inscribe successively four interferograms to achieve the strain $\epsilon_T = 4 \cdot 10^{-3}$. Corresponding to the specimen yield point since under the assumptions made each interferogram overlaps a strain range of $(0\text{-}1.26) \cdot 10^{-3}$. To study the kinetics of specimen deformation up to its rupture, around 200 interferograms must be inscribed. It is conceivable that the solution of such problems is associated with the development of methods for an automated survey of the experimental information and the creation of algorithms for its processing on an electronic computer. At the present time no such serially produced automated complexes for processing holographic interferograms exist, but there is research in this area [27-29].

3. DETERMINATION OF THE STRAIN STATE OF THE SECTION OF AN ARTICLE SURFACE BEING STUDIED

One hologram inscribed by the method of two exposures contains all the information necessary to analyze changes in the strain state of the article surface being studied, which occurred therein in the time interval between the two exposures. By recording four interference pattern from four pairwise symmetrical directions relative to the z axis and using the dependences (2.1)-(2.4), we determine the functions U(x, y), V(x, y), W(x, y). Since holographic interferometry only determines small strain (see (2.7)), then the components ϵ_x, ϵ_y, γ_{xy} of the strain tensor are found according to the Cauchy relationships [30]

$$\varepsilon_x = \partial U/\partial x,\ \varepsilon_y = \partial V/\partial y,\ \gamma_{xy} = \partial U/\partial y + \partial V/\partial x \tag{3.1}$$

by numerical or graphical differentiation of the functions U and V found experimentally. The quasiprincipal strains $\epsilon_{1,2}$ on the article surface and their orientation are found from the formulas

$$\varepsilon_{1,2} = \frac{1}{2}\left((\varepsilon_x + \varepsilon_y) \pm \sqrt{(\varepsilon_x - \varepsilon_y)^2 + \gamma_{xy}^2}\right); \tag{3.2}$$

$$\operatorname{tg} \alpha_1 = 2(\varepsilon_1 - \varepsilon_x)/\gamma_{xy} \tag{3.3}$$

(α_1 is the angle between the direction of the principal strain ϵ_1 and the x axis).

The strain $\epsilon_z = \partial W/\partial z$ is not determined successfully directly by the holographic interferometry method. Only the two partial derivatives $\partial W/\partial x$ and $\partial W/\partial y$ can be found from the experimental data and taking account of the fact that the load free areas of the article external surface are principal, two more partial derivatives $\partial V/\partial z = -\partial W/\partial y$, $\partial U/\partial z = -\partial W/\partial x$, which when known it is possible to extrapolate the behavior of the functions U and V in the subsurface layer of the object being studied. The strain ϵ_z is obtained in terms of the strains ϵ_x and ϵ_y:

$$\varepsilon_z = -\mu^*(\varepsilon_x + \varepsilon_y)/(1 - \mu^*), \tag{3.4}$$

where $\mu^* = 0.5 - (1-2\mu)E_c/2E$ [31]; E, μ are the elastic modulus and Poisson ratio of the article material, $E_c = \sigma_0/\epsilon_0$ is the secant modulus on the strain curve, $\sigma_0 = \sigma_i = \sqrt{\sigma_x^2 - \sigma_x\sigma_y + \sigma_y^2 + 3\tau_{xy}^2}$ is the stress intensity, $\varepsilon_0 = \varepsilon_i + (1-2\mu)\sigma_i/E$,

$$\varepsilon_i = \frac{\sqrt{2}}{3}\sqrt{(\varepsilon_x - \varepsilon_y)^2 + (\varepsilon_y - \varepsilon_z)^2 + (\varepsilon_z - \varepsilon_x)^2 + 1.5\gamma_{xy}^2} \tag{3.5}$$

Fig. 6

is the strain intensity. Thus, in order to find the strain ϵ_z, it is necessary to construct first a generalized strain curve $\sigma_i = f(\epsilon_i)$ for the material of the article being studied and the dependence of the variable elasticity parameter μ^* on ϵ_i but we cannot use these dependences directly since ϵ_z is unknown and therefore so is ϵ_i. To overcome this difficulty, two means can be used: 1) taking account of the insignificant influence of the Poisson ratio on the stress distribution, to set $\mu = 0.5$, i.e., to consider the material incompressible; 2) to use the method of succcssive approximations: giving $\mu_1^* = 0.5$, finding $\epsilon_i^{(1)}$ by the dependence (3.5) and by the graph of $\mu^* = f_1(\epsilon_i)$ the new value μ_2^* and later continuing the process until $|\mu_n^* - \mu_{(n-1)}^*| < \Delta$ (Δ is the accuracy taken for convergence of the approximations). This latter recipe, in particular, can be utilized even to determine the limits between the elastic and plastically deformed zones of the article material [32].

One of the known plasticity conditions (Tresk or Mises) or one of the known models of plasticity (Henke–Il'yushin deformation theory, St.-Venant–Mises, and Prandtl–Reiss flow theories) must be used in going over to an analysis of the stress state.

As already mentioned, HIM can be used only for step-by-step methods of recording information. Consequently, the dependences (3.1)-(3.4) actually determine the increments in the strain components in the alternate stage of article loading. Depending on the selection of the points on the strain curve corresponding to the first and second exposures of the photographic material, the unstored interference fringe patterns will carry information about the strain increments corresponding to either active loading or unloading or residual molding of the article [11, 33].

4. EXPERIMENTAL RESULTS

Analysis of the Strain State of a Plate from the D16T Alloy with a Central Circular Hole Under Uniaxial Tension. The geometric dimensions of the specimen under investigation and the strain patten of the article material are presented in Fig. 1. The tensile force is oriented along the axis of symmetry that agrees with the y axis. Before the tests the specimen surface was treated with a fine abrasive paper to approximate the shape of the scattering index to a spherical one. The holograms were inscribed on photographic plates LOI-2 fastened to the specimen surface by using SKTN-A rubber and developed in dilute (1:10) Petrov developer [34]. The light source was a LG-38 He–Ne laser. The specimen tests were performed on a DM-30 testing machine; weak green illumination was maintained in the room when recording the holograms. The loading process was checked by PKB 10-100 strain gauges glued by TsIAKRIN-ÉO glue (two remote from the concentrator and two near the danger points at the hole contour). The points on the strain diagram correspond to loading stages and recording of two-exposure holograms.

Starting with the sixth step, the force on the specimen dropped after termination of the loading process (the final steady value of the load is indicated in Fig. 1). The second exposure was only realized when the rate of force drop became practically zero.

Presented in Figs. 2a-c are photographs corresponding to the first (P = 2.8 kN, ΔP = 2.8 kN), fifth (P = 10.9 kN, ΔP = 1.2 kN), and eighth (P = 12.4 kN, ΔP = 0.5 kN) loading stages (P is the total load and ΔP its increment in the stage).

Quantitative decoding of the holographic interferograms was performed for the first five stages. Strain fields $\varepsilon_x(x, y)$, $\varepsilon_y(x, y)$, $\gamma_{xy}(x, y)$ were constructed. Shown in Fig. 3 is the distribution of the strain ϵ_y at different sections x = const in the fifth stage of specimen loading.

Setting $\mu^* = 0.5$, ϵ_i was determined and then σ_i was found from the generalize strain curve (see Fig. 1). The beginning of the plastic deformation of the material was determined from the Mises condition $\sigma_i = \sigma_T$. For our case $\sigma_T = 333$ MPa, $\epsilon_i = 6.67 \cdot 10^{-3}$. Presented in Fig. 4 are σ_y diagrams for the degree of plastic deformation $\psi = 0.687$ obtained by the theory of small elastic–plastic deformations 1 and the St.-Venant–Levi–Mises theory 2 (the agreement of the diagrams is satisfactory as it indeed should be under simple loading) and the residual stress diagram 3 in the danger section of the specimen as the computed difference of diagrams, one of which is obtained experimentally while the other is calculated by formulas of elasticity theory 4 under the assumption of ideal elasticity of the article material [35].

Construction of a Strain Diagram at the Most Loaded Point of a Plate with a Hole under Low-Cycle Loading. Specimens were fabricated from D16T sheet material. The geometric dimensions of the specimen and the kind of coordinate grid superposed on its surface are represented in Fig. 5a. To prevent specimen buckling under compression, its working section was reduced to a minimum and was 70-80 mm (the distance between loading unit clamps). Specimen loading was performed in a UMÉ-10TM machine. The maximal load on the specimen did not exceed 80 kN. The elements of the installation optical scheme (the LG-38 laser, lenses, irises, etc.) are arranged side by side on an ordinary laboratory table. A sign-variable load is applied to the specimen. Twenty-three holographic interferograms were recorded in the first loading cycle. A dependence of the strain amplitude on the amplitude of the sign-varying load P applied to the specimen (Fig. 5b) is constructed according to the calculated values of ϵ_y at the point A with coordinates $x = R$, $y = 0$.

Analogously 22 holograms were obtained after 350 cycles of soft symmetric specimen loading with load amplitude of 80 kN. The strain diagram of the specimen material in the 351st loading cycle at the point A is presented in Fig. 5c. A comparison of the curves in Figs. 5b and c shows that the alloy D16T hardens. The curve in Fig. 5d, whose external view corresponds to the elastic nature of material work at this point, corresponds to the strain diagram of the specimen material at the point B.

For a quantitative estimate of the Bauschinger effect, Mazing proposed that the sum of the stresses at which unloading started $\sigma^{(0)}$ and $\sigma_T^{(1)}$ (a new proportionality limit) under reverse loading a constant quantity, equal twice the proportionality limit in the initial loading:

$$\sigma^{(0)} + \sigma_T^{(1)} = S_T^{(1)} = 2\sigma_T^{(0)}. \tag{4.1}$$

In our case $\sigma^{(0)} \approx 222$ MPa, $\sigma_T^{(1)} \approx 55$ MPa, $S_T^{(1)} \approx 278$ MPa, $\sigma_T^{(0)} \approx 140$ MPa, i.e., the relationship (4.1) is satisfied with good enough accuracy.

Recording of Relaxation Processes in the Alloy D16T. A thick plate with a circular concentrator was subjected to plastic deformation in the zone of a hole by means of a steel continuous cylinder whose diameter was approximately three times the diameter of the hole. After removal of the load, a 1.6-mm depression was formed in the plate. By using a three-point contact the hologram of such a deformed surface was recorded in real time in opposing beams. After several days, the interference fringe pattern that had appeared in this time interval (Fig. 6) was photographed. The different nature of the molding inside and outside the deformed zone is clearly traced in strips of finite width on the photograph. The normal displacement of the inner zone was around 0.5 μm.

LITERATURE CITED

1. R. Sharpe (ed.), Nondestructive Testing Methods [Russian translation], Mir, Moscow (1972).
2. R. K. Erff (ed.), Holographic Nondestructive Investigations [in Russian], Mashinostroenie, Moscow (1979).
3. D. Casesent (ed.), Optical Information Processing [Russian translation], Mir, Moscow (1980).
4. A. B. Kudrin, P. I. Polukhin, and N. A. Chichenev, Holography and Deformation of Metals [in Russian], Metallurgiya, Moscow (1982).
5. C. West, Holographic Interferometry [Russian translation], Mir, Moscow (1982).
6. A. G. Kozachok, Holographic Methods of Investigation in Experimental Mechanics [in Russian], Mashinostroenie, Moscow (1984).

7. R. Jones and K. Wakes, Holographic and Speckle-Interferometry [Russian translation], Mir, Moscow (1986).
8. V. G. Seleznev, A. N. Arkhipov, and T. V. Ibragimov, "Application of holographic interferometry to determine residual stresses," Zavod. Lab., 42, No. 6 (1976).
9. V. G. Seleznov, A. N. Arkhipov, and T. V. Ibragimov, "Determination of residual stresses that are variable along the rod length by a holographic interferometry method," Zavod. Lab., 43, No. 9 (1977).
10. V. V. Yakovlev and V. P. Shchepinov, "Determination of residual strains at a crack apex by a holographic interferometry method," Coll. Scient. Work Chelyab. Polytech. Inst., No. 182 [in Russian] (1976).
11. V. P. Shchepinov and V. V. Yakovlev, "Determination of elastic–plastic strain components by a holographic interferometry method," Zh. Tekh. Fiz., 49, No. 5 (1979).
12. V. P. Shchepinov and V. V. Yakovlev, "Investigation of the deformation process of articles by a holographic interferometry method," Zh. Prikl. Mekh. Tekh. Fiz., No. 6 (1979).
13. V. V. Yakovlev, V. P. Shchepinov, and P. N. Odintsov, "Investigation of the initial residual strains in articles by a holographic interferometry method," Probl. Prochn., No. 10 (1979).
14. V. A. Khandogin, "Applications of coherent optics methods of measurement to the solution of certain problems of crack theory (survey)," Holographic Measuring Systems [in Russian], NETI, Novosibirsk (1980).
15. V. I. Arkhipov, "Field of elastic–plastic strains in the area of a crack mouth," Zh. Prikl. Mekh. Tekh. Fiz., No. 4 (1980).
16. M. I. Tselikov, B. A. Morozov, et al., "Application of holographic interferometry to study the elastic and plastic deformation process," Probl. Prochn., No. 6 (1976).
17. Residual Stresses and Regulation Methods [in Russian], IPM Akad. Nauk SSSR, Moscow (1983).
18. Residual Technological Stresses [in Russian], IPM, Akad. Nauk SSSR, Moscow (1985).
19. M. Lothar, "Ermittlung plastischer Verfommngen mit Hilfe der holografischen Interferometrie," FMC-Ser. Inst. Mech. Akad. Wiss. DDR, No. 3 (1982).
20. I. V. Volkov, "Investigation of the kinetics of plastid deformation by a holographic method," Uch. Zap., TsAGI, 15, No. 2 (1984).
21. V. A. Zhilkin and L. A. Borynyak, "Holographic interferometry method using Denisyuk holograms to investigate the strain state of an object," Physical Principles of Holography. Materials of the Second All-Union School on Holography [in Russian], Leningrad Nuclear Physics Inst., USSR Acad. Sci., Leningrad (1979).
22. V. A. Zhilkin and S. I. Gerasimov, "On the possibility of studying the strain state of articles by using an applied interferometer," Zh. Tekh. Fiz., 52, No. 10 (1982).
23. D. B. Neumann and R. C. Penn, "Object motion compensation using reflection holography (A)," J. Opt. Soc. Am., 62 (1972).
24. Yu. N. Denisyuk, "On mapping of optical properties of an object in the wave field of the radiation it scattered," Dokl. Akad. Nauk SSSR, 144, No. 6 (1962).
25. P. M. Boone, "Use of reflection holograms in holographic interferometry and speckle correlation for measurement of surface displacements," Optica Acta, 22 (1975).
26. G. S. Pisarenko, A. P. Yakovlev, and V. V. Matveev, Handbook on Strength of Materials [in Russian], Naukova Dumka, Kiev (1975).
27. V. I. Guzhov, A. I. Druzhinin, et al., "Measuring–calculating system to investigate the stress–strain state of objects," Avtometriya, No. 4 (1982).
28. N. A. Marchenko and A. Kh. Pergament, Processing Interferograms on an Electronic Converter [in Russian], Preprint No. 42, Inst. Prikl. Mat. Akad. Nauk SSSR (1982).
29. S. I. Gerasimov, V. I. Guzhov, et al., "Automation of interference pattern processing in the investigation of strain fields," Zavod. Lab., 51, No. 4 (1985).
30. G. S. Pisarenko and N. S. Mozharovskii, Equations and Boundary Value Problems of Plasticity and Creep Theories [in Russian], Naukova Dumka, Kiev (1981).
31. I. A. Birger and R. R. Mavlyutov, Strength of Materials [in Russian], Nauka, Moscow (1986).
32. A. Ya. Aleksandrov and M. Kh. Akhmetzyanov, Polarization Optic Methods of the Mechanics of a Deformable Body [in Russian], Nauka, Moscow (1973).
33. V. A. Zhilkin and A. M. Popov, "Holographic Moire method," Zavod. Lab., 45. No. 11 (1979).

34. V. D. Petrov, "High-speed processing of photographic layers when obtaining reflection holograms," Zh. Nauch. Prikl. Fotogr., 21, No. 3 (1976).
35. I. A. Birger, Residual Stresses [in Russian], Mashgiz, Moscow (1963).

TRANSMISSION OF A SHOCK LOAD BY BULK MEDIA

B. E. Gel'fand, S. P. Medvedev, A. N. Polenov, and S. M. Frolov

UDC 532.593

The sliding of an air-borne shock wave (ASW) over the surface of a dust layer was studied in [1]. It was shown that the character of the change in pressure on the base in the presence of the layer differs significantly from the propagation of an ASW along a pure surface. In view of the practical importance of this phenomenon, here we conduct a detailed experimental investigation of the parameters of a compression wave acting on a rigid wall covered by layers of different bulk materials during shock loading. We examine both cases of normal incidence of the ASW on the layer and propagation of the ASW along the surface of the layer.

1. Normal Incidence of an ASW on the Layer. Experiments were performed on a vertical shock tube with an inside diameter of 50 mm and a length of 3 m. A diagram of the experimental unit is shown in Fig. 1a. The high-pressure chamber (HPC) 1, with a length of 1.5 m, was separated from the low-pressure chamber (LPC) 2 by a membrane 3. The LPC was equipped with piezoelectric pressure sensors 4-6. Layers of bulk materials were placed on the end of the LPC with a built-in sensor 6. Table 1 shows the characteristics of the test substances (ρ_p, ρ_n, φ, and d are respectively the density of the material of the particles, the bulk density and volume concentration of the solid phase, and the mean size of the particles). We used sized screens to scatter the particles. The piezoelectric sensors were of the LKh type. The diameter of the sensitive surface was 1 cm, which was much greater than d. The sensor 5 was placed near the surface of the layer, while the sensor 4 served as the triggering sensor. The HPC contained nitrogen or helium, while the LPC contained air at a pressure $p_0 = 0.1$ MPa. The signals from the sensors were recorded on S8-17 oscillographs. The excess pressure on the front of the incident SW's $\Delta p = p_1 - p_0$ (p_1 is the pressure behind the shock front) was varied within the range 0.05-1 MPa.

The experiments showed that in shock loading, the character of pressure on the end covered by the bulk material differs from the familiar case of the interaction of an ASW with a rigid wall. After reflection of the incident ASW from the free surface of the bulk medium, a pressure disturbance arrives at the end underneath the layer. This disturbance characterizes the surge at the front of the shock wave and the subsequent decrease in pressure – with rapidly decaying oscillations – to the pressure associated with reflection of the wave on the surface of the layer p. The duration of the surge in pressure is proportional to the height of the layer, while its amplitude may be several times greater than the "steady" value of p. The latter value is slightly (by 10-20%) less than the pressure associated with reflection on a rigid wall.

In isolated cases, we attempted to explain the nature of the above phenomenon by obtaining measurements using the scheme in Fig. 1b. This scheme allowed us to distinguish the effects of the solid and gas phases on the character of the pressure record. Two sensors were located at the end of the shock tube. Sensor 1 was placed in direct contact with the particles of the bulk medium (i.e. as sensor 6). The sensitive surface of sensor 2 was covered by a perforated barrier to exclude contact with the particles but permit penetration of the gas. Tests showed that the presence of the barrier did not affect the character of the pressure record if it was positioned near the sensitive surface of the sensor.

Figure 2a and b shows the pressure record in the experiments conducted by the scheme in Fig. 1b, with a layer of substance 3 (see Table 1) having a height h = 20 mm. The time scale

Moscow. Translated from Zhurnal Prikladnoi Mekhaniki i Tekhnicheskoi Fiziki, No. 2, pp. 115-121, March-April, 1988. Original article submitted December 25, 1986.

 0021-8944/88/2902-0268$12.50